JOURNAL OF MATERIALS SCIENCE **38** (2003) 1057–1061

Crystalline structure and dielectric properties of $Ba(Ti_{1-y}Ce_y)O_3$

ZHI JING
Department of Ceramics and Glass Engineering, University of Aveiro, 3810 Aveiro, Portugal

ZHI YU
Materials Research Laboratory, The Pennsylvania State University, University Park, PA 16802, USA

CHEN ANG*
Department of Physics, The University of Akron, Akron, OH 44325, USA

Crystalline structure, microstructure and dielectric properties for $Ba(Ti_{1-y}Ce_y)O_3$ ($0 \leq y \leq 0.5$) ceramics have been studied. Dense ceramics with the relative density higher than 95% and grain size of 0.7–1.5 μm have been obtained. The limit of the solid solubility is determined as $y = \sim 0.3$ by the X-ray diffraction, SEM, and dielectric properties measurements. The crystalline symmetry is tetragonal for the sample with $y = 0.02$ and cubic for $y \geq 0.06$ at room temperature, and the unit cell increases with increasing Ce content in the solid solution range. Correspondingly, the dielectric response exhibits three dielectric peaks for $y = 0.02$, and one pinched dielectric peak with ferroelectric relaxor behavior for $y \geq 0.06$.

1. Introduction

$BaTiO_3$ is a typical ferroelectric material that has been extensively studied both theoretically and experimentally on its dielectric, ferroelectric and piezoelectric properties, phase transitions, etc [1]. One of the interesting features in doped $BaTiO_3$ is the so-called ferroelectric-relaxor behavior. In the last two decades, many efforts have been devoted to explore the physical nature of the ferroelectric-relaxor behavior [2–5]. However, some details of the dynamics of dielectric response are still not clear. Although the ferroelectric relaxor behavior was first observed in Sn doped $BaTiO_3$ by Smolenskii *et al.* [6, 7] many studies on the ferroelectric-relaxor behavior are currently focused on Pb-based compounds, such as $Pb(Mg_{1/3}Nb_{2/3})O_3$, $Pb(Sc_{1/2}Ta_{1/2})O_3$ and $(Pb,La)(Zr,Ti)O_3$ [2–5]. A reason for the difficulty in understanding of the ferroelectric-relaxor behavior was attributed to the complicated crystalline structure of the Pb-based compounds [8, 9]. In fact, many doped $BaTiO_3$ systems show an obvious ferroelectric-relaxor behavior and possess simple crystalline structure. From this point view, the doped $BaTiO_3$ system might be a good model material for exploring the physical nature of the ferroelectric-relaxor behavior.

On the other hand, through doping with different elements in $BaTiO_3$, the ferroelectric properties of $BaTiO_3$ can be greatly adjusted in order to meet different demands for applications [10], for example, as an important material for making ceramic capacitors [11–14], and as a lead-free material for high actuator applications [15–17]. Among $BaTiO_3$-base materials, the ferroelectric properties of Ce doped $BaTiO_3$ have recently received much attention due to both the fundamental and application interests [12–14]. In the previous study of Ce doped $BaTiO_3$ [18, 19], the present authors briefly reported the synthesis and ferroelectric-relaxor behavior of some compositions for $Ba(Ti_{1-y}Ce_y)O_3$ ceramics. In this paper, we extend the compositions to lower Ce concentration, and report a detail study of the phase assemblages, crystalline structure, microstructure, and ferroelectric-relaxor behavior of the $Ba(Ti_{1-y}Ce_y)O_3$ ceramics.

2. Experimental procedure

$Ba(Ti_{1-y}Ce_y)O_3$ ceramics with $y = 0$, 0.02, 0.06, 0.1, 0.2, 0.3, 0.33, 0.4, and 0.5 were synthesized by the mixed oxide method. Raw materials $BaCO_3$(>99.5%, May & Baker Ltd.), CeO_2 (>99.99%, Johnson Matthey GmbH) and TiO_2 (>99.8%, Johnson Matthey GmbH) were weighed according to the nominal composition. The mixtures were wet mixed in alcohol on a planetary mill with agate balls for 6 hours and calcined at 1200°C for 4 hours. The calcined powders were milled again for 6 hours. After drying, the powders were isostatically pressed into disks under 300 MPa. Finally, the disks were sintered in air at 1530°C–1550°C for 6 hrs and furnace cooled.

*Author to whom all correspondence should be addressed.

The X-ray diffraction (XRD) analysis was carried out to determine the phase assemblage and lattice parameters of the samples by using Cu K_α radiation (Rigaku) at room temperature, with 2θ angles between 20° and 100° and the scanning speed of 1°/min. The microstructure of the polished and thermally etched sections of samples was observed via scanning electron microscopy (SEM) (Hitachi 4100).

The silver electrodes were pasted and then fired at 650°C. The dielectric properties were measured with a Keithley 3330 LCZ Meter and a Solartron 1260 Impedance Analyzer at 0.1, 1, 10, and 100 kHz in the temperature range 12–500 K under an ac field of 1 V/mm.

3. Results and discussion

3.1. Phase assemblage and crystalline structure

The XRD patterns of the $Ba(Ti_{1-y}Ce_y)O_3 (0 \leq y \leq 0.5)$ samples are shown in Fig. 1. Single phase $Ba(Ti_{1-y}Ce_y)O_3$ solid solutions were identified for $y \leq 0.3$, within the XRD resolution. For the sample with $y = 0.33$, besides the main phase $BaTiO_3$, an additional weak peak appeared, which was identified to be probably CeO_2 phase. The samples with $y = 0.4$ and 0.5 were found to be composed of multiphases $BaTiO_3$, $BaCeO_3$ and CeO_2. These XRD results give the first evidence that the solid solubility of Ce^{4+} at Ti ions in $BaTiO_3$ lattice is at about 30 at.%.

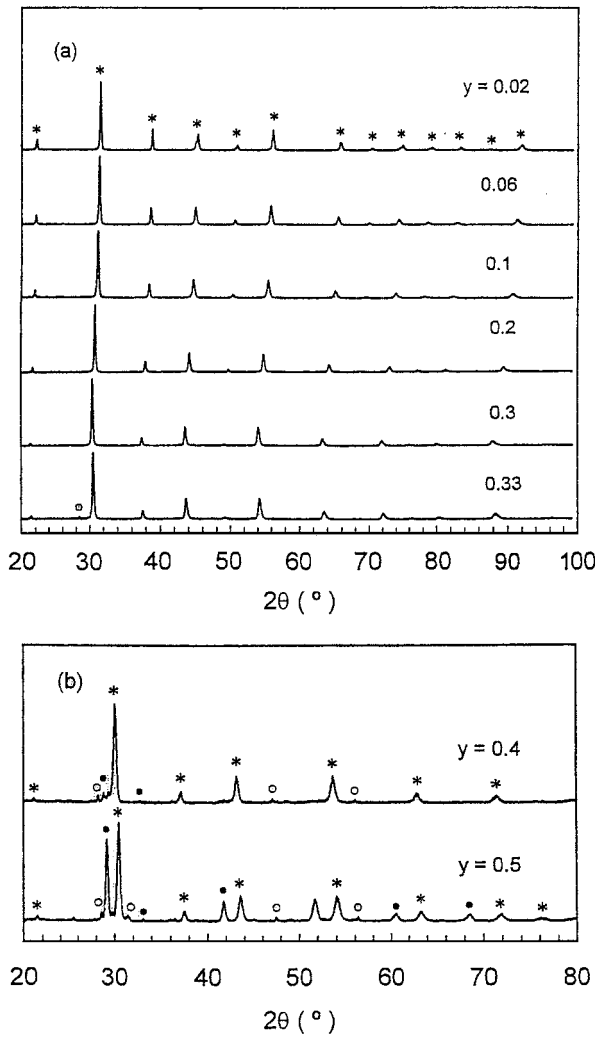

Figure 1 XRD patterns of the $Ba(Ti_{1-y}Ce_y)O_3$ ($0 \leq y \leq 0.33$) ceramics. ∗ main phase; ○ extra phase.

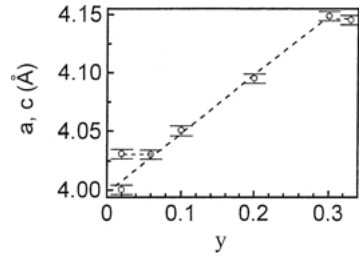

Figure 2 The lattice parameters (a and c) versus y for the $Ba(Ti_{1-y}Ce_y)O_3$ ceramics.

Lattice parameters were calculated by the least square method. The variation of the lattice parameters as a function of Ce concentrations is shown in Fig. 2. In the present work, the sample with $y = 0.02$ can be well indexed with a tetragonal symmetry. However, the samples with $y \geq 0.06$ are better indexed by a cubic symmetry. The lattice parameter of the samples with $y \geq 0.06$ increases monotonically with increasing Ce content in the range $0.06 \leq y \leq 0.3$, but almost constant for $y \geq 0.3$, which confirms that the solid solubility of Ce^{4+} at Ti sites in $BaTiO_3$ is about 0.3.

It should be pointed out that Ce ions can also substitute for Ba sites. Whether Ce ions enter Ba sites or Ti sites depends mainly on two facts: (1) the Ba/Ti ratio, and (2) the sintering temperature and atmosphere. In our study it was found that it is difficult to control which sites Ce will be located at for the Ce content below 1 at.%. However, above 1 at.% doping level, the substitution site of Ce ions can be controlled well by adjusting Ba/Ti ratio and sintering temperatures in air. For example, as Ba/Ti <1 and sintering the samples below 1480°C in air, Ce substitutes for Ba sites, and the solubility is 8 at.%, which is consistent with the report in the literature [20]. As Ba/Ti > 1 and the samples were sintered above 1530°C in air, Ce ions mainly substitute for Ti sites, as we observed in this work.

3.2. Microstructure and grain size

The microphotographs of the polished and thermally etched sections of the $Ba(Ti_{1-y}Ce_y)O_3$ samples are shown in Fig. 3a–h. The microstructure of the ceramics is uniform and dense. Single-phase solid solutions have been obtained for the samples with $y \leq 0.3$. For $y = 0.4$ and 0.5, the ceramic samples are clearly multiphasic. However, for $y = 0.33$, only a small amount of second phase was occasionally identified (probably being CeO_2 as determined by XRD in Fig. 1a), which was more clearly shown by the combination of the back scattered and secondary electron images (as shown in Fig. 4). Thus, the SEM microphotographs also show that the solid solubility of Ce^{4+} at Ti sites in $BaTiO_3$ is about 30 at.%, which is in agreement with the results of XRD patterns analysis and lattice parameter calculation.

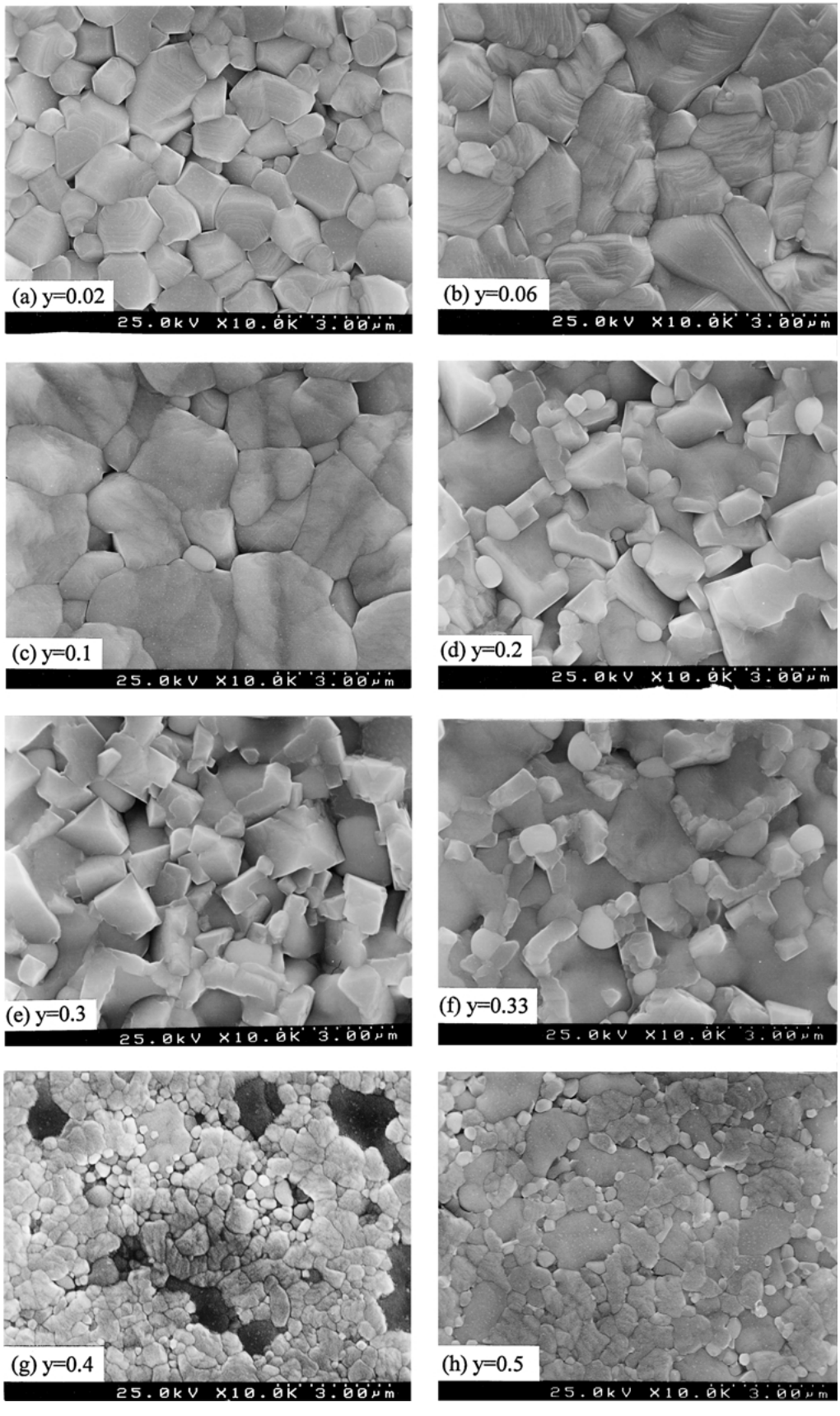

Figure 3 SEM micrographs of the polished sections of the $Ba(Ti_{1-y}Ce_y)O_3$ ceramics with (a) $y = 0.02$, (b) $y = 0.06$, (c) $y = 0.1$, (d) $y = 0.2$, (e) $y = 0.3$, (f) $y = 0.33$, (g) $y = 0.4$ and (h) $y = 0.2$ sintered at 1530–1550°C for 6 hours.

The average grain size of the samples was calculated from the SEM microphotographs. Fig. 5 shows the average grain size as a function of Ce content for the $Ba(Ti_{1-y}Ce_y)O_3$ solid solutions. The average grain size ranges from 0.7 to 1.5 μm.

4. Dielectric properties and discussion

The temperature dependence of the dielectric constant (ε) at 10 kHz for the $Ba(Ti_{1-y}Ce_y)O_3$ system with $y = 0$–0.3 is shown in Fig. 6. For undoped $BaTiO_3$ ($y = 0$), sharp phase transitions are observed at 402 K,

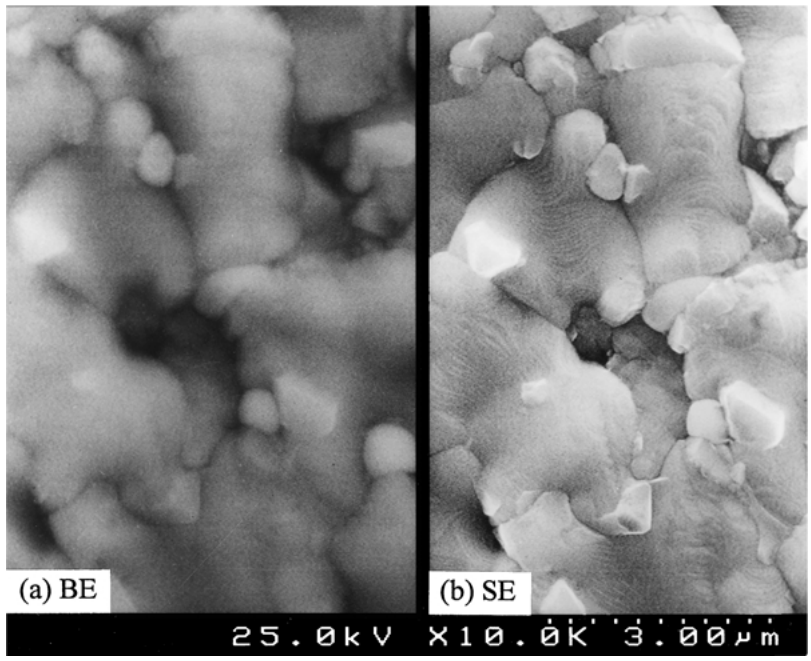

Figure 4 The back scattered and secondary electron images of the polished sections of the $Ba(Ti_{1-y}Ce_y)O_3$ sample with $y = 0.33$.

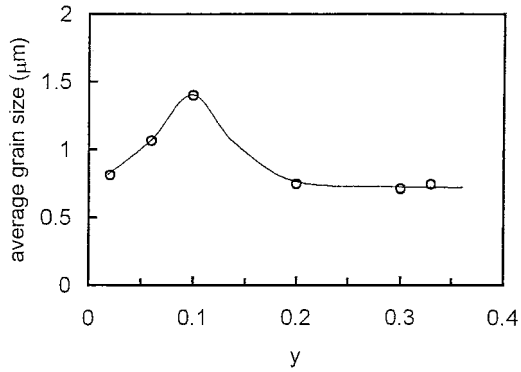

Figure 5 The average grain size versus y for the $Ba(Ti_{1-y}Ce_y)O_3$ ceramics.

285 K and 204 K, corresponding to the paraelectric (cubic)—ferroelectric (tetragonal) phase transition (denoted as T_c), ferroelectric phase transitions from tetragonal to orthorhombic structure (T_1) and from orthorhombic to rhombohedral structure (T_2), respectively. For the sample with $y = 0.02$, which shows a tetragonal symmetry at room temperature, the three

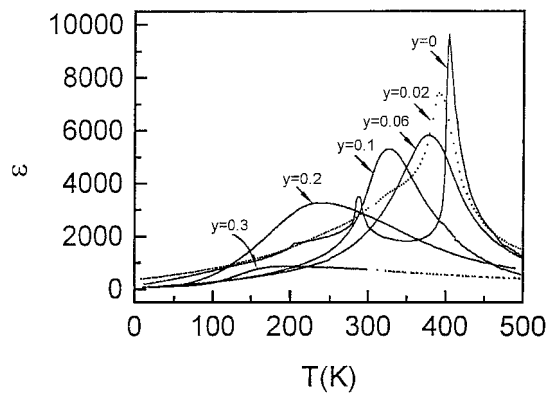

Figure 6 The temperature dependence of the dielectric constant at 10 kHz for the $Ba(Ti_{1-y}Ce_y)O_3$ solid solutions.

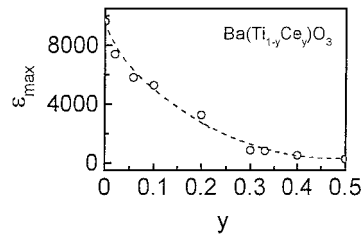

Figure 7 The dielectric constant maximum (ε_m) at 10 kHz versus y for the $Ba(Ti_{1-y}Ce_y)O_3$ samples.

phase transitions are observed, similar to that of pure $BaTiO_3$, however ε peaks are shifted with T_c to a lower temperature and T_1 and T_2 to higher temperatures. The samples are cubic symmetry when $y \geq 0.06$, and only one rounded ε peak is observed. Obviously, the variation of the dielectric behavior is closely related to the change in the crystalline structure, which was modified by Ce doping.

The variation of the dielectric constant maximum (ε_m) at 10 kHz as a function of Ce concentration y is shown in Fig. 7. ε_m decreases continuously with increasing Ce concentration until $y = 0.3$ and keeps almost constant for $y > 0.3$. This is due to the solid solubility of Ce^{4+} at Ti-sites of $BaTiO_3$ being at about $y = 0.3$. However, it should be pointed out that ε is generally sensitive to the grain size and density of doped $BaTiO_3$ ceramics. The relative density for the ceramic samples with $y \leq 0.3$ was higher than 95%.

The temperature dependence of ε for the samples as a function of frequency has been also measured. For the samples doped with low Ce concentration, almost no frequency dependence was observed. However, rounded ε peaks are observed with obvious frequency dispersion for the samples with $y \geq 0.1$. The representative temperature dependence of ε as a function of frequency for the sample with $y = 0.2$ is shown in Fig. 8. The rounded ε peak with frequency dispersion

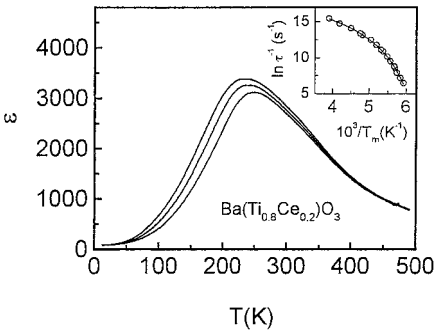

Figure 8 The temperature dependence of the dielectric constant for the $Ba(Ti_{1-y}Ce_y)O_3$ sample with $y = 0.2$ at 1, 10, and 100 kHz (from top to bottom). Inset: the relaxational times τ versus temperatures (circles: experimental data; solid curve: fit to the Vogel–Fulcher relation).

is well developed. The relaxational times (τ) were obtained from the frequency dependence of the imaginary part of the complex-permittivity. The temperature dependence of τ is plotted in the inset of Fig. 8. The result shows that τ follows the Vogel–Fulcher relation [21],

$$\tau = \tau_0 \exp[U/k_B(T - T_{VF})] \qquad (1)$$

where τ_0 is the pre-exponential term, E is the hindering barrier, T_{VF} is the Vogel-Fulcher temperature and k_B is the Boltzmann constant. The fitting curve is shown in the inset of Fig. 8, with the fitting parameters $\tau_0 = 9.24 \times 10^{-9}$ s and $T_{VF} = 139$ K. It is known that the relaxation rate following the Vogel–Fulcher relation is a typical characteristic of ferroelectric relaxor. The result indicates that the sample with $y = 0.2$ exhibits a typical ferroelectric-relaxor behavior. The similar behavior for the samples with $y = 0.1$ and 0.3 was also observed.

5. Conclusions

In this work, detailed results on the crystalline structure, microstructure and dielectric behavior of the $Ba(Ti_{1-y}Ce_y)O_3$ system have been reported. The main results are,

1. The solid solubility of Ce^{4+} at Ti sites in $Ba(Ti_{1-y}Ce_y)O_3$ is ~30 at.%. At room temperature, the crystal symmetry changes from tetragonal to cubic with increasing Ce within the solubility limit. The $Ba(Ti_{1-y}Ce_y)O_3$ ceramics with the relative density higher than 95% have been obtained. The average grain size is in the range of 0.75 μm to 1.5 μm.

2. With partially substitution of Ce^{4+} at Ti ions, the crystalline structure of $BaTiO_3$ is changed from a tetragonal symmetry for $y = 0.02$ to a cubic symmetry for $y \geq 0.06$ at room temperature, and the unit cell increases with increasing Ce concentration within the solid solution range. Correspondingly, the dielectric response exhibits three dielectric peaks for $y = 0.02$, and one pinched dielectric peak with ferroelectric-relaxor behavior for $y \geq 0.06$. That is, a crossover from the ferroelectric to ferroelectric-relaxor behavior occurred with increasing Ce concentration in the $Ba(Ti_{1-y}Ce_y)O_3$ solid solutions.

Acknowledgments

The authors thank Prof. J. L. Baptista for his stimulating discussion. ZHI Jing thank the PRAXIS XXI, FCT (Portuguese Foundation for Science and Technology) for financial support.

References

1. B. JAFFE, W. COOK and H. JAFFE, in "Piezoelectric Ceramics" (Academic Press, London, 1971).
2. X. YAO, Z. L. CHEN and L. E. CROSS, *J. Appl. Phys.* **54** (1984) 3399.
3. L. E. CROSS, *Ferroelectrics* **76** (1987) 241.
4. D. VIEHLAND, S. J. JANG, L. E. CROSS and M. WUTTIG, *J. Appl. Phys.* **68** (1990) 2916.
5. V. WESTPHAL, W. KLEEMANN and M. D. GLINCHUK, *Phys. Rev. Lett.* **68** (1992) 847.
6. G. A. SMOLENSKII and V. A. ISUPOV, *Zh. Tekhn. Fiz.* **24** (1954) 1375.
7. G. A. SMOLENSKI, *J. Phys. Soc. Jpn. Suppl.* **28** (1970) 26.
8. J. TOULOUSE, B. E. VUGMEISTER and R. PATTNAIK, *Phys. Rev. Lett.* **73** (1994) 3467.
9. CHEN ANG, ZHI YU, P. LUNKENHEIMER, J. HEMBERGER and A. LOIDL, *Phys. Rev.* B **59** (1999) 6670.
10. F. JONA and G. SHIRANE, "Ferroelectric Crystals" (Dover Publication, New York, 1993).
11. ZHI JING, CHEN ANG, ZHI YU, P. M. VILARINHO and J. L. BAPTISTA, *J. Appl. Phys.* **84** (1998) 983; *J. Amer. Ceram. Soc.* **82** (1999) 1345.
12. D. F. K. HENNINGS, B. SCHREINEMACHER and H. SCHREINEMACHER, *J. Europ. Ceram. Soc.* **13** (1994) 81.
13. Y. PARK and Y. KIM, *J. Mater. Res.* **10** (1995) 2770.
14. D. MAKOVEC, Z. SAMARDAIJA and D. KOLAR, *J. Solid State Chem.* **123** (1996) 30; *J. Amer. Ceram. Soc.* **80**(1) (1997) 45.
15. S. WADA, S. SUZUKI, T. NOMA, T. SUZUKI, M. OSADA, M. KAKIHANA, S. E. PARK, L. E. CROSS and T. R. SHROUT, *Jpn. J. Appl. Phys.* **38** (1999) 5505.
16. ZHI YU, RUYAN GUO and A. S. BHALLA, *Appl. Phys. Lett.* **77** (2000) 1535.
17. *Idem.*, *J. Appl. Phys.* **88** (2000) 410.
18. CHEN ANG, ZHI YU, ZHI JING, P. M. VILARINHO and J. L. BAPTISTA, *J. Euro. Ceram. Soc.* **17** (1997) 1217.
19. ZHI YU, CHEN ANG, ZHI JING, P. M. VILARINHO and J. L. BAPTISTA, *J. Phys.: Condens. Matter* **9** (1997) 3081.
20. ZHI JING, ZHI YU and CHEN ANG, *J. Mater. Res.* accepted for publication.
21. H. VOGEL, *Z. Phys.* **22** (1921) 645; G. Fulcher, *J. Amer. Ceram. Soc.* **8** (1925) 339.

Received 25 July 2001
and accepted 9 September 2002